

## Freezing in Ising ferromagnets

V. Spirin, P. L. Krapivsky, and S. Redner

Center for BioDynamics, Center for Polymer Studies, and Department of Physics, Boston University, Boston, Massachusetts 02215

(Received 3 May 2001; revised manuscript received 6 September 2001; published 18 December 2001)

We investigate the final state of zero-temperature Ising ferromagnets that are endowed with single-spin-flip Glauber dynamics. Surprisingly, the ground state is generally *not* reached for zero initial magnetization. In two dimensions, the system reaches either a frozen stripe state with probability  $\approx 1/3$  or the ground state with probability  $\approx 2/3$ . In greater than two dimensions, the probability of reaching the ground state or a frozen state rapidly vanishes as the system size increases; instead the system wanders forever in an isoenergy set of metastable states. An external magnetic field changes the situation drastically—in two dimensions the favorable ground state is always reached, while in three dimensions the field must exceed a threshold value to reach the ground state. For small but nonzero temperature, relaxation to the final state proceeds first by formation of very long-lived metastable states, as in the zero-temperature case, before equilibrium is reached.

DOI: 10.1103/PhysRevE.65.016119

PACS number(s): 64.60.My, 05.50.+q, 75.40.Gb

### I. INTRODUCTION

#### A. Background

Despite extensive study [1,2], basic questions about the kinetic Ising model with Glauber dynamics remain unanswered [3]. In this paper, we investigate the following: What is the final state of a finite Ising-Glauber spin system when it is quenched from infinite temperature to zero temperature [4]? An infinite system organizes into a coarsening domain mosaic of up and down spins, with the characteristic length scale growing as  $t^{1/2}$  [2]. For a finite system, this coarsening stops when the typical domain size reaches the system size  $L$ . Intriguingly, such a system typically gets stuck in an infinitely long-lived metastable state. In two dimensions, this probability of getting stuck is approximately  $1/3$  as  $L \rightarrow \infty$ , while for  $d \geq 3$  the ground state is essentially never reached.

To provide context about the ultimate fate of the Ising-Glauber system, consider the limiting cases of  $d=1$  and  $d=\infty$ . For a linear chain of length  $L$  with  $pL$  up spins and  $(1-p)L$  down spins, the final state of the system follows from two simple facts. First, the average magnetization is conserved under Glauber dynamics [1,5] and, second, the only possible final states are all spins up or all spins down; there are no metastable states in one dimension. For the final magnetization to equal the initial magnetization, a fraction  $p$  of all realizations must therefore end with all spins up (and fraction  $1-p$  must end with all spins down). Thus the probability  $P(p)$  to ultimately have all spins up is simply  $P(p)=p$ . A very different result holds in the mean-field limit. For this limit, consider the complete graph, in which each spin interacts equally with every other spin. For any nonzero magnetization, it is energetically favorable for any minority spin to flip so that the majority phase quickly fills the system for  $p \neq 1/2$ . Therefore  $P(p)$  is simply the step function  $P(p)=\theta(p-1/2)$ .

In two and higher dimensions, the probability that one phase eventually “wins” also converges to a step function in  $p-1/2$ , but with strange anomalies when  $p=1/2$ . A two-dimensional system has a nonzero probability of getting stuck in a metastable state that consists of two or more straight stripes. In greater than two dimensions, the probability that the ground state is reached vanishes quickly with

increasing system size [4]. The final state is also not static, but consists of stochastic “blinkers.” These are localized spins that can flip without any energy cost. The system wanders *ad infinitum* on a connected set of equal-energy states defined by these blinkers. In the categorization proposed by Newman and Stein [3], when  $d \geq 3$  the Ising system is of the “mixed” type, because a fraction of the spins flips a finite number of times, while the complementary fraction flips infinitely often.

Imposition of an external magnetic field gives rise to bootstrap percolation phenomena for the evolution of the spins [6,7]. On the square lattice, an infinitesimal field is sufficient to drive the system to the energetically favorable ground state. This corresponds to  $n=3$  bootstrap percolation on this lattice [6,7]. On the cubic lattice, the energetically favorable ground state is reached only if the field exceeds a threshold value. For weaker fields, a transition between phase coexistence and field alignment occurs as a function of the initial concentration of field-aligned spins. This transition again can be described in terms of  $n=4$  bootstrap percolation on the cubic lattice.

At low positive temperatures the aforementioned metastable states continue to play a significant role in the relaxation toward equilibrium. For example, in  $d=2$  and for temperatures up to approximately  $0.2T_c$ , there is a large time range for which the relaxation is close to that of the zero-temperature system. If a metastable stripe configuration happens to form, a time of the order of  $L^3 e^{4J/T}$  must elapse, where  $J$  is the interaction strength between spins, before the system can escape this metastable state and reach equilibrium. Similarly, metastable states will influence the long-time relaxation even more strongly in higher dimensions.

#### B. The model

We study the homogeneous ferromagnetic Ising model with Hamiltonian  $\mathcal{H} = -J \sum_{\langle ij \rangle} \sigma_i \sigma_j$ , where  $\sigma_i = \pm 1$ , and the sum is over all nearest-neighbor pairs of sites  $\langle ij \rangle$ . Spins are initially uncorrelated, corresponding to initial temperature  $T_i = \infty$ . This limit implies that the fractions of up and down spins are equal. Because we are interested in fluctuation effects associated with zero initial magnetization  $m_0$ , we prepare our systems with fixed magnetization rather than fixed

probability for each spin orientation. Thus every initial configuration has  $L^d/2$  up spins and  $L^d/2$  down spins for  $m_0 = 0$ , and  $pL^d$  up spins and  $(1-p)L^d$  down spins for  $m_0 = 2p - 1 \neq 0$ .

The spins evolve by zero-temperature Glauber dynamics [1], i.e., the system is quenched from an initial temperature  $T_i = \infty$  to  $T = 0$ . For each initial configuration, one realization of the dynamics was performed until the final state was reached. We consider  $d$ -dimensional hypercubic lattices with linear size  $L$  and periodic boundary conditions. Most of our results continue to hold for free boundary conditions and on other even-coordinated lattices. (On odd-coordinated lattices stable convex islands of minority spins readily form and the system always freezes into a disordered state [3,4].)

Glauber dynamics at zero temperature is implemented by picking flippable spins at random and computing the energy change  $\Delta E$  if this spin were to flip. Flippable spins are those with  $\Delta E \leq 0$ . For  $\Delta E < 0$  or  $\Delta E = 0$ , respectively, the spin flip is accepted with probability 1 or 1/2. After each such event, the time is incremented by 1/(number of flippable spins). Thus in one time unit each spin attempts one flip on average.

The rest of this paper is organized as follows. In Sec. II we discuss various geometric properties of the final state in two and three dimensions, including the influence of an external magnetic field on the final state, as well as the distributions of final state magnetization and energy. The number of metastable states as a function of the spatial dimension is estimated in Sec. III to illustrate the increasing influence of metastable states as the dimension increases. In Sec. IV, we discuss the finite-temperature evolution in two dimensions and argue that the zero-temperature metastable states continue to play a significant role even when the system is quenched to a temperature  $T \approx 0.2T_c$ . Section V gives a summary and discusses some open questions.

## II. FINAL STATE GEOMETRY

We first study  $P(p)$ , the probability that an Ising system with  $pL^d$  up spins initially, which is quenched to  $T = 0$ , ultimately has all spins up. One could imagine three possible outcomes: (1)  $P(p)$  is a monotonically increasing function of  $p$ . (2)  $P(p) = 0$  for  $0 \leq p \leq p_c$ ;  $P(p)$  increases monotonically for  $p_c < p < 1 - p_c$ ;  $P(p) = 1$  for  $p_c \leq p \leq 1$ . (3)  $P(p)$  is the step function  $P(p) = \theta(p - 1/2)$ .

In one dimension the first case applies. We argue that in higher dimensions the third case is realized. If so, then additional considerations are needed to determine  $P(1/2)$ . The behavior at  $p = 1/2$  is particularly interesting because the concentrations of up and down spins are equal for any initial temperature that exceeds the critical temperature,  $T_c < T_i \leq \infty$ , as long as the magnetic field is zero. Naively, one might expect that the system always reaches one of the ground states in the thermodynamic limit. Up-down symmetry then implies  $P(1/2) = 1/2$ . Surprisingly, this hypothesis is incorrect for all spatial dimensions  $d \geq 2$ . A two-dimensional system does not always reach the ground state, while for  $d \geq 3$  the system never reaches the ground state as  $L \rightarrow \infty$ .

The crucial difference between one and higher dimensions

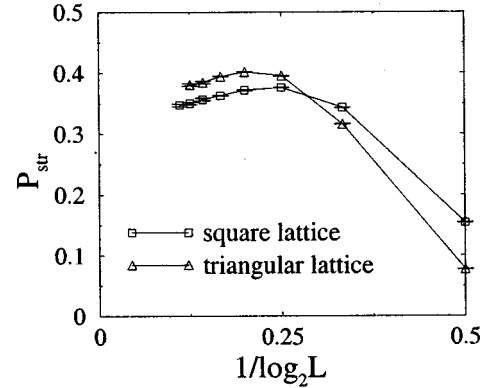


FIG. 1. Probability that an  $L \times L$  system ( $\square$  square lattice,  $\Delta$  triangular lattice) eventually reaches a stripe state,  $P_{\text{str}}(L)$ , as a function of  $1/\log_2 L$  for  $L$  up to 512. Each data point, with error bars smaller than the size of the symbol, is based on  $\geq 10^5$  initial spin configurations.

is that there are numerous metastable states for  $d > 1$  and no such states for  $d = 1$ . Metastable states are easily visualized in two dimensions, where any straight stripe of width  $\geq 2$  that traverses the entire system is stable at zero temperature [4,8]. Metastable states are geometrically more complex in three and higher dimensions, as will be discussed in Sec. II B.

### A. Two dimensions

#### 1. Stripe state in zero magnetic field

Our simulations indicate that a system with zero initial magnetization reaches a stripe state with nonzero probability as  $L \rightarrow \infty$  (Fig. 1). Linear extrapolation of the last four data points for the probability of reaching the stripe state,  $P_{\text{str}}(L)$ , versus  $L$  gives  $P_{\text{str}}(\infty) \approx 0.315$  and 0.344 on the square and triangular lattices, respectively. While an arbitrary even number of stripes is possible, we typically obtain two stripes of similar widths for a square system. Metastable states with more than two stripes rarely appear. For example, the probability of reaching the four-stripe state grows slowly with  $L$  but is less than 0.07% for  $L = 200$ .

We can understand qualitatively the dependence of the probability of obtaining  $k$  vertical stripes in the final state,  $P_v(k, A)$ , by analyzing an  $AL \times L$  rectangular system and then taking the  $L \rightarrow \infty$  limit. For example, for aspect ratio  $A = 9$  and  $L = 32$ , the final probabilities  $P_v(k, A)$  in  $10^4$  realizations are 0.0028, 0.101, 0.351, 0.359, and 0.152, for  $k = 0, 2, 4, 6$ , and 8. There is also a probability 0.034 for a horizontal stripe. In general, the probability  $P_v(k, A)$  is peaked around  $k_{\text{max}} \propto A$ . Invoking the assumption of analyticity in  $A$  then implies that the probabilities  $P_v(k, A)$  of  $k$ -stripe states are positive for all even  $k$  and arbitrary aspect ratio  $A$ .

Our data also qualitatively suggest that  $P_v(k, A)$  decays faster than exponentially in  $k$ . This is analogous to the behavior of the number of spanning clusters on large but fixed aspect ratio rectangles at the percolation threshold. In that problem, it has been recently shown that the number of span-

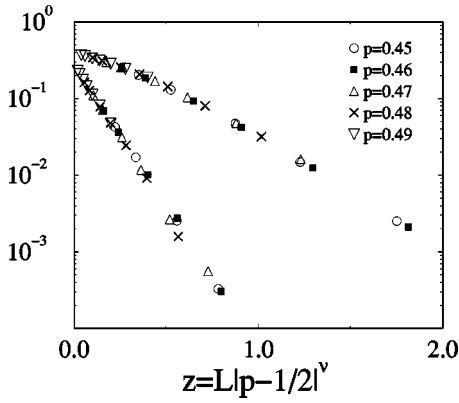


FIG. 2. Probability that the minority phase wins,  $\mathcal{M}(z)$  (lower), or that a stripe state is reached,  $\mathcal{S}(z)$  (upper) as a function of  $L|p-1/2|^\nu$ , with  $\nu=1.5$  and  $\nu=1.35$ , respectively. Data are based on systems with  $L \leq 200$  and  $\geq 5 \times 10^4$  initial configurations.

ning clusters is greater than 1 [11,12]. We now employ an argument similar to that of Ref. [12] to estimate the large- $k$  behavior of  $P(k,A)$ .

Consider the probability  $P_h(k,A)$  of reaching a state with  $k$  horizontal stripes. Now divide the rectangle into two thinner rectangles each of size  $AL \times L/2$ . In the large- $k$  limit, the dominant contribution to  $P_h(k,A)$  comes from situations where approximately  $k/2$  stripes traverse each of the rectangles. This argument implies  $P_h(k,A) \sim [P_h(k/2,2A)]^2$ , which may be iterated to give

$$P_h(k,A) \sim [P_h(2, Ak/2)]^{k/2}. \quad (1)$$

The quantity  $P_h(2, Ak/2)$  is the probability to have a horizontal stripe in a rectangle of dimension  $AL \times 2L/k$ . If we take  $L \sim k$  as the original rectangle width, then the subdivided rectangle  $AL \times 2L/k$  has a width of order 1. For such a narrow rectangle, a stripe can occur only if it existed initially. This clearly occurs with probability  $2^{-2L} = 2^{-Ak}$ . Thus, substituting  $P_h(2, Ak/2) \sim e^{-Ak}$  into Eq. (1), we deduce that

$$P_h(k,A) \sim e^{-\text{const} \times Ak^2}. \quad (2)$$

That is,  $P_h(k,A)$  has a Gaussian tail and states with a large number of stripes are extremely rare.

For a small initial magnetization, an Ising system is dominated by the majority phase. To quantify this we study (i) the probability  $\mathcal{M}(p,L)$  that the minority phase wins, that is, the sign of the magnetization in the final (ground) state is opposite to that in the initial state, and (ii) the probability  $\mathcal{S}(p,L)$  that the system reaches a stripe state. Both quantities exhibit scaling when  $L \rightarrow \infty$  and initial magnetization  $m_0 \rightarrow 0$ , with the combination  $z \equiv L|2p-1|^\nu$  held constant.

The best data collapse is achieved with  $\nu \approx 1.5$  and  $\nu \approx 1.35$ , respectively, for  $\mathcal{M}$  and  $\mathcal{S}$ . Further,  $\mathcal{M}(z)$  appears to decay exponentially in  $z$  while  $\mathcal{S}(z)$  decays more quickly (Fig. 2). The exponential behavior for  $\mathcal{M}$  can be inferred by considering the limiting case of  $p \rightarrow 0$ . Here a minority spanning cluster exists with probability  $\propto p^L$  from which  $\mathcal{M}(z)$  also decays exponentially with  $z$ . Therefore in two dimensions the initial majority phase always “wins” as  $L \rightarrow \infty$  and

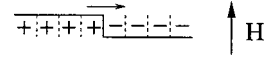


FIG. 3. In a weak positive field an interface kink can move only to the right, while in zero field this kink diffuses.

$P(p) = \theta(p-1/2)$ , just as in the mean-field limit. Thus we expect that  $P(p)$  is a step function for all spatial dimensions  $d \geq 2$ .

## 2. Finite magnetic field

An external magnetic field  $H$  strongly affects the fate of the system. On the square lattice and for  $H > 2J$  (strong field), down spins that have three aligned neighbors can now flip parallel to the field and the system necessarily ends up in the field-aligned ground state. Conversely, for  $0 < H < 2J$  (weak field), only the dynamics of spins that have two misaligned neighbors is modified. In zero field such spins flip with rate  $1/2$ , while in a weak field they flip parallel to the field with rate 1. This means that kinks on interfaces move in only one direction rather than diffusing (Fig. 3).

The most interesting case is that of weak field and small initial concentration of up spins. The system consists of small clusters of up spins in a background of down spins. Due to the unidirectional motion of kinks on interfaces, clusters of up spins can grow until each fills out its convex hull (Fig. 4). If the convex hull of one cluster overlaps with either another up cluster or its convex hull, then the resulting aggregate can expand further to fill out this enlarged convex hull. If there is yet another cluster (or convex hull) within this expansion zone, growth continues.

This growth is closely related to bootstrap percolation [6], in which a lattice is occupied at initial density  $\rho_0$ , and then all sites that do not have at least  $n$  occupied neighbors are removed. This deletion is repeated until no more sites can be removed. The case  $n=3$  is closely related to our weak-field system, with spins antiparallel to the field playing the role of occupied sites in bootstrap percolation. In  $n=3$  bootstrap percolation, all occupied sites will eventually be removed for  $L \rightarrow \infty$ , even if  $\rho_0$  is arbitrarily close to 1. Translating this to the Ising system, we conclude that for any nonzero concentration of up spins the system will evolve to the spin-up ground state.

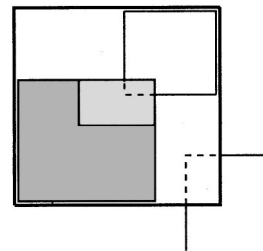


FIG. 4. Expansion of a cluster of up spins (dark shaded) in a weak magnetic field  $H < 2J$ . The convex hull (union of dark and light shaded regions) overlaps with the cluster on the upper right. The convex hull of this aggregate (outer rectangle) then overlaps with yet another cluster on the lower right, leading to continued expansion.

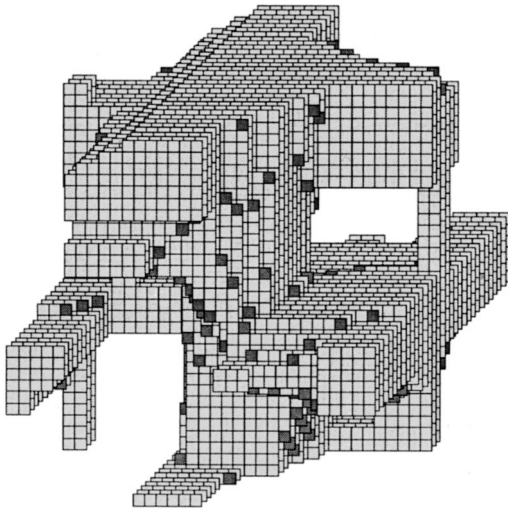


FIG. 5. Typical final state on a  $32^3$  cubic lattice with periodic boundary conditions. Spins of one phase are indicated by small blocks. The dark shaded spins can flip freely and are part of blinker states.

**B. Three dimensions**

*1. Blinkers in zero magnetic field*

On the simple cubic lattice, the structure of the final state is surprisingly complex. A representative example is shown in Fig. 5. In the figure, each spin occupies a unit cube (only one phase is shown). For nearly all initial states with initial concentration of up spins  $p = 1/2$  (much greater than the percolation threshold  $p_c \approx 0.3116$  [7]), the final state consists of only two clusters, each of which percolates in all three coordinate directions. For example, for  $L = 20, 30,$  and  $40$ , the probability that both phases percolate in all three directions equals  $0.83, 0.92,$  and  $0.97$ , respectively. The number of distinct spin clusters almost always equals 2—there are no small clusters of spins.

Generically, this cluster consists of a core three-arm star [Fig. 6(a)], augmented with several straight filaments. The three-arm star permits two clusters of oppositely oriented spins, each devoid of convex corners, to percolate in all three directions. Each arm is oriented along one coordinate direc-

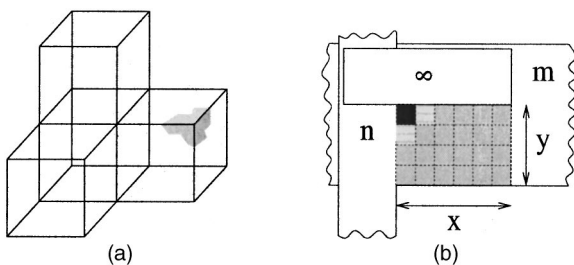


FIG. 6. (a) A three-arm star consisting of four cubic blocks of linear dimension  $L/2$  in an  $L \times L \times L$  system with periodic boundary conditions. The other phase occupies the remainder of the volume. A convex corner (for free boundary conditions) is shown shaded. (b) Stochastic blinker on the cubic lattice. The shaded region of size  $x \times y \times (n - m)$  contains a fluctuating interface which can range between all spins up and all spins down.

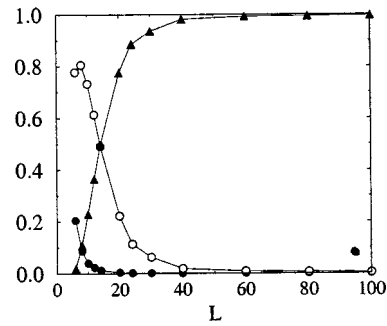


FIG. 7. Probability that the system reaches the ground state (dots), a frozen metastable state (circles), or a blinker state (triangles) as a function of the linear dimension. The number of realizations is  $\geq 10^4$  for each system size. The lines are a guide for the eye.

tion and joins onto itself so that there are no convex corners. This is the three-dimensional analog of stripes on the square lattice.

Another striking feature of the final state is the presence of stochastic blinker spins that reside in convex corners. The typical geometry of such blinkers is shown in Fig. 6(b). Here we view the percolating cluster of up spins as a building with an  $m$ -story section (marked  $m$ ), an adjacent  $n$ -story section (with  $n > m$ ), and a section (marked  $\infty$ ) that wraps around the torus in the vertical direction and rejoins the building on the ground floor. The wiggly lines indicate wrapping around the torus in the  $x$  and  $y$  directions. Thus the arms of this three-arm star cannot shrink under Glauber kinetics. The shaded portion of Fig. 6(b) supports a blinker. This blinker starts at the upper left corner of the shaded region of height  $m$ , where it costs zero energy to flip the heavy shaded spin. Once this spin flips, its three nearest neighbors [two light shaded and one just above the dark shaded spin in Fig. 6(b)] can also flip with no energy cost. Continuing this process gives rise to a fluctuating interface in the shaded parallelepiped that is bounded by the states of all spins up and all spins down. Thus a blinking state wanders forever by transitions between connected metastable configurations with the same energy.

Because of the pervasiveness of blinker states, the probability of reaching either the ground state or a frozen metastable state decreases rapidly with increasing system size (Fig. 7). In fact, we find that the ground state is never reached in  $5 \times 10^4$  realizations for  $d = 3$  systems with linear dimension  $L \geq 60$ . The fact that the final state is usually a blinker leads to a subtlety in deciding when the “final” state has actually been reached. For  $d \geq 3$ , the energy evolves by small decrements separated by increasingly long plateaus. These plateaus are indicative of blinkers and it is not *a priori* obvious if a plateau extends forever or if it will be terminated by an energy decrement. As a time-saving measure, we consider that the final state has been reached when a simulation reaches  $1.1\tau$ , where  $\tau$  is the time of the most recent energy decrement. We verified on medium-size systems that changing the stopping criterion to  $5\tau$  had a negligible influence on the value of the final energy. This ambiguity in the stopping

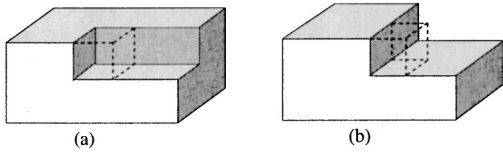


FIG. 8. (a) Cluster of up spins with a concave trough. The trough is sequentially filled in, for  $0 < H < 2J$ , by flipping spins that each have three misaligned neighbors. The dashed cube indicates the spin that is about to flip. (b) Cluster of up spins with a concave interface. The energy cost of flipping the indicated spin is  $4J - 2H$ ; thus, this spin will flip when  $H > 2J$ .

time also leads to a larger uncertainty in the final magnetization, which is proportional to the fraction of blinker sites.

## 2. Finite magnetic field

An external magnetic field again drastically changes the final state of the system. On the cubic lattice there are now two critical field,  $H_1 = 2J$  and  $H_2 = 4J$ , which demarcate different behaviors. A weak field  $0 < H < 2J$  modifies the dynamics of spins that have three misaligned neighbors—now they can only flip to align with the field. These spins, when flipped, fill in concavities and eventually complete convex corners, as illustrated in Fig. 8(a). This weak-field regime also corresponds to  $n=4$  bootstrap percolation on the cubic lattice [6], where again clusters of spins antiparallel to the field correspond to occupied sites in the percolation problem. Numerically we find that there is a threshold initial concentration of up spins,  $p_H$ , below which finite droplets of up spins, with each spin having at least three aligned neighbors, freeze. For  $p > p_H$ , the infilling of concavities leads to repeated mergings of clusters of up spins and the ground state is ultimately reached. Our simulations give  $p_H \approx 0.25$ , distinctly less than the site percolation threshold  $p_c \approx 0.3116$ .

The intermediate-field regime  $2J < H < 4J$  corresponds to  $n=5$  bootstrap percolation on the cubic lattice. Here it is possible for a spin adjacent to a straight but concave interface to flip [Fig. 8(b)]. This filling ultimately allows a cluster of up spins to systematically expand and fill its convex hull. This then leads to a picture similar to the  $n=3$  bootstrap on the square lattice, namely, the coalescence of convex hulls of neighboring clusters leads to a final state where all spins are aligned with the field for any initial magnetization. Finally, in the strong-field regime ( $H > 4J$ ), even a single up spin nucleates the growth of additional up spins and the system quickly reaches the ground state with all spins pointing up.

## C. Final magnetization and energy distributions

The magnetization and energy distributions are important physical characteristics of the final state. While we have no theoretical understanding of these distributions, numerically we find that these quantities exhibit intriguing behaviors. We hope that these results will trigger future theoretical work.

In two dimensions, we have found that either the ground state or a stripe state, typically with two stripes of approximately the same width, is reached. This qualitative observation can be made more precise by studying the magnetization

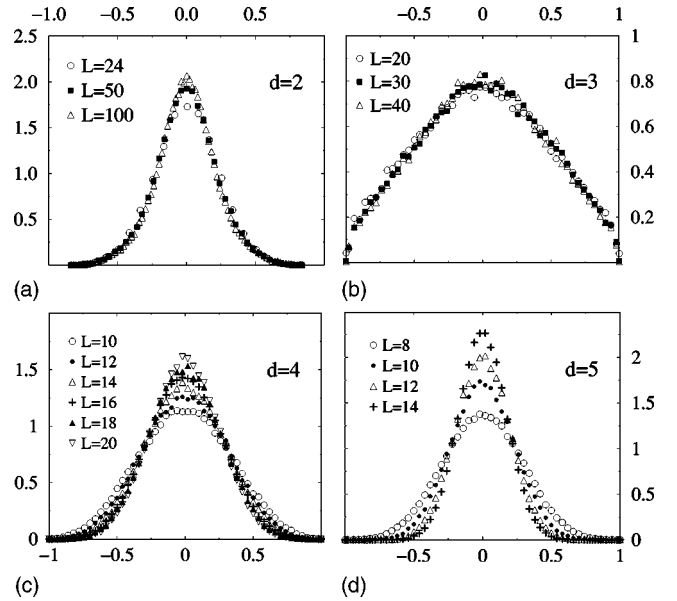


FIG. 9. Final magnetization distribution versus  $m$  in 2–5 dimensions. The number of configurations is  $\geq 10^5$  for all system sizes in  $d=2, 4$ , and  $5$ , and  $\geq 5 \times 10^4$  in  $d=3$ . In  $d=2$ , the  $\delta$ -function peaks at  $m = \pm 1$  have been suppressed.

distribution of the final state. Configurations that reach the ground state give  $m = +1$  or  $-1$ , while configurations that reach the stripe state lead to a continuous component of the magnetization distribution [Fig. 9(a)]. The width of this peak gradually narrows as the system size increases but converges to a nonzero limit as  $L \rightarrow \infty$ .

For  $d \geq 3$ , the probability of reaching the ground state is vanishingly small so that there is only the continuous component of the magnetization distribution. For  $d=3$ , the distribution is much broader than in two dimensions [Fig. 9(b)], with evidence of singular behavior as  $|m| \rightarrow 1$ . Based on much less data, we previously suggested [4] that the magnetization distribution could be fitted by the form  $3(1 - m^2)/4$ . This hypothesis now seems to be incorrect.

We also simulated the magnetization distribution for  $d > 3$  and find that it becomes systematically narrower as the dimension increases [Figs. 9(c) and 9(d)]. The width of the magnetization distribution appears to approach zero as a power law  $L^{-\nu}$ , where  $\nu \approx 0.44$  in  $d=4$  and  $\nu \approx 0.94$  in  $d=5$ .

In two dimensions, the distribution of final energy  $P(E, L)$  is a series of  $\delta$ -function peaks at energies  $E = 4n/L$ , with  $n$  a non-negative integer; these correspond to configurations with  $2n$  stripes. Here  $E$  is the energy per spin in units of  $J$  (with  $E=0$  the ground state energy). Conversely, for  $d \geq 3$ , the distribution  $P(E, L)$  becomes smooth in the thermodynamic limit since the separation between adjacent energies decreases as  $L^{-d}$ .

In  $d=3$ , the energy distribution exhibits single-parameter scaling,  $P(E, L) = \langle E \rangle^{-1} \mathcal{P}(E/\langle E \rangle)$ , where  $\langle E \rangle$  is the average energy per spin (Fig. 10). We find that  $\langle E \rangle$  decays as  $L^{-\chi}$ , with the exponent  $\chi$  in the range  $0.85$ – $0.90$ . Thus the total energy of the final state, which is proportional to the total interfacial area, grows as  $L^{3-\chi} \approx L^{2.1}$ . This is consistent with

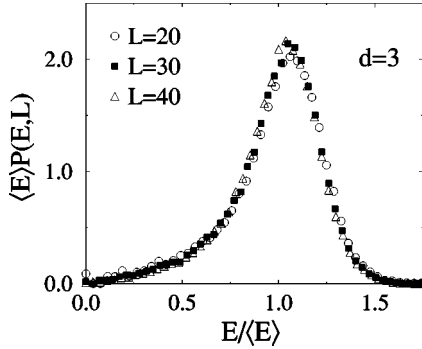


FIG. 10. Scaled distribution of final energy per spin in  $d=3$ . The number of configurations is  $\geq 5 \times 10^4$  for all system sizes.

the qualitative picture for the geometry of the final state given in Fig. 5.

In higher dimensions, the energy distribution apparently exhibits two scales (Fig. 11)—the average energy  $\langle E \rangle$  and the width  $w \equiv \langle (E - \langle E \rangle)^2 \rangle^{1/2}$ , which decays faster in  $L$  than  $\langle E \rangle$  itself. In other words,  $P(E, L) = w^{-1} \mathcal{P}[(E - \langle E \rangle)/w]$ . The average energy per spin appears to approach the ground state energy according to the power law  $\langle E \rangle \sim L^{-\chi}$ , with  $\chi \approx 0.5$  in  $d=4$  and  $\chi \approx 0.4$  in  $d=5$ .

### III. NUMBER OF METASTABLE STATES

The fact that the kinetic Ising system with Glauber kinetics is more likely to get stuck in a metastable state in  $d=3$  compared to  $d=2$  suggests that such states become systematically more numerous as  $d$  increases. It is therefore instructive to determine the number of metastable states as a function of the spatial dimension. On the square lattice these metastable states are simply related to the ground state of a one-dimensional Ising model with competing interactions. For  $2 < d < \infty$ , we give a simple lower bound for the number of metastable states which shows that such states become more prevalent as  $d$  increases. Finally, we compute the number of metastable states on a three-coordinated Cayley tree as an estimate for the number of metastable states when  $d = \infty$ .

#### A. Finite dimensions

It is easy to verify that the metastable states of the ferromagnetic Ising-Glauber model on an  $L \times L$  square lattice with periodic boundary conditions consist of purely vertical or horizontal stripe arrays, with the width of each stripe

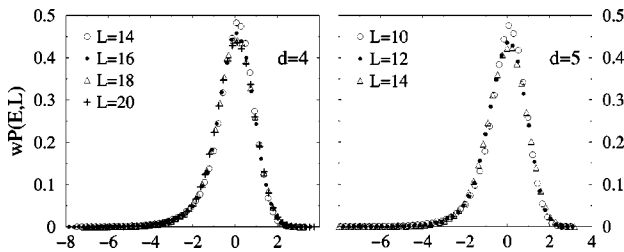


FIG. 11. Scaled distribution of final energy per spin in  $d=4$  and  $5$  as a function of  $(E - \langle E \rangle)/w$ . The number of configurations is  $\geq 10^5$  for all system sizes.

greater than or equal to 2. As discussed in [4], these states are essentially identical to the ground states of the axial next-nearest-neighbor Ising (ANNNI) chain with nearest-neighbor ferromagnetic interaction  $J_1$  and second-neighbor antiferromagnetic interaction  $J_2$  when  $J_2 = -J_1/2$  [13]. For a chain of  $L$  sites, the number of ground states on the linear chain grows asymptotically as  $g^L$ , where  $g = (1 + \sqrt{5})/2$  is the golden ratio. Consequently, the number of metastable states on a square of  $\mathcal{N} = L^2$  sites asymptotically scales as  $M_2(\mathcal{N}) \sim e^{B_2 \sqrt{\mathcal{N}}}$ , where  $B_2 = \ln g = 0.48121 \dots$

Metastable states are geometrically more complex in greater than two dimensions (Fig. 5). However, a simple lower bound for the number of such states can be readily established by considering the higher-dimensional analog of the stripe states. In three dimensions, for example, this class of metastable states consists of an array of straight filaments of general cross-sectional shape, with the constraints that the linear dimension of any feature must be  $\geq 2$  and that the separation between any two filaments in either coordinate direction is also  $\geq 2$ . The number of such filament states in three dimensions clearly scales as  $\exp(C_3 \mathcal{N}^{2/3})$ , and the generalization to  $d$  dimensions gives  $\exp(C_d \mathcal{N}^{1-1/d})$  as a lower bound to the number of metastable states  $M_d(\mathcal{N})$ . Exact enumeration of all the metastable states for  $d \geq 3$  appears to be a tantalizing combinatorial problem. We believe that  $\ln M_d(\mathcal{N}) \propto \mathcal{N}^{1-1/d}$ , i.e., the lower bound provides qualitatively correct asymptotic behavior.

#### B. Infinite spatial dimension

For infinite spatial dimension, we estimate the number of metastable states by considering the Cayley tree. The Cayley tree is pathological because a finite fraction of sites are on the surface, but it has the virtue of being tractable. We shall exactly enumerate all the metastable states on the Cayley tree and show that their number scales as  $\exp(C_\infty \mathcal{N})$ , as expected from the lower bound from the previous subsection. It is also worth mentioning the alternative of considering either random graphs [14] or “thin” graphs [15] to model infinite spatial dimension. Both these types of graph are random and the latter additionally satisfy the constraint that every site is connected with a *fixed* number of other sites. On the random graph system, numerical simulations show that an Ising system on this graph tends to freeze into a metastable state for intermediate values of coordination number [14]. On thin graphs, a computation of the number of metastable states [15] yields a qualitatively similar result to that of the Cayley tree.

For the Cayley tree, there is a subtlety that depends on the coordination number being even or odd. While odd-coordinated lattice systems exhibit the pathology of metastable freezing for any initial magnetization, even-coordinated lattices naturally give rise to blinker states. Since we are interested in the number of metastable states, we consider only the three-coordinated tree. The fact that the Ising system on this tree necessarily freezes into a glassy final state fits with our expectation for what occurs on  $d$ -dimensional hypercubic lattices as  $d \rightarrow \infty$  [16].

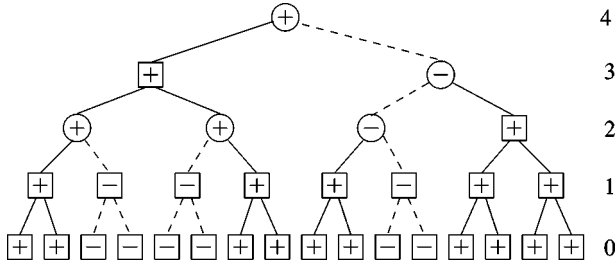


FIG. 12. A typical metastable state on a three-coordinated Cayley tree. Circled spins are those whose state is determined by its parent one level higher while boxed spins are uniquely determined by the states of the daughter spins. Clusters of negative spins are joined by dashed lines.

We consider the three-coordinated tree with root at level  $N$  (Fig. 12). Two nodes in level  $N-1$  attach to the root site, then four nodes form level  $N-2$ , etc. To enumerate the number of metastable states  $M_N$  on an  $N$ -level tree, first note that there are two types of spin in any metastable state. For a spin at level  $n$ , if the two daughter spins in level  $n-1$  agree, then the state of the parent spin is uniquely determined. Conversely, if the daughters disagree, then the state of the spin in level  $n$  (circled in Fig. 12) is determined by that of its parent in level  $n+1$ . (The neighboring spins at level 0 must agree.)

Let  $D_N$  and  $U_N$  be the number of metastable states with the root spin determined and undetermined by their daughters, respectively. By enumerating all possible daughter states and the outcome of the root site, we find that  $D_N$  and  $U_N$  obey the recursion relations

$$D_{N+1} = \frac{1}{2} D_N^2 + \frac{1}{2} U_N^2 + 2 D_N U_N, \quad (3)$$

$$U_{N+1} = D_N^2, \quad (4)$$

subject to the initial conditions  $D_0=0$  and  $U_0=2$ . For example, the recurrence (4) expresses the fact that the root spin is undetermined only when two daughter spins are uniquely determined and of opposite sign. Thus  $U_{N+1} = 2 \times D_N \times \frac{1}{2} D_N$ , where the factor 2 accounts for the fact that the root spin remains undetermined and the factor  $\frac{1}{2}$  ensures that the root spins in the daughter trees are oppositely oriented.

From the first few terms in these recursion formulas, we see that  $U_N$  and  $D_N$  grow very rapidly with increasing  $N$ . To obtain their asymptotic behavior, we divide Eq. (3) by  $U_{N+1}$  and use Eq. (4) to find the following recursion relation for  $\Lambda_N = D_N/U_N$ :

$$\Lambda_{N+1} = \frac{1}{2} + \frac{2}{\Lambda_N} + \frac{1}{2\Lambda_N^2} \equiv R(\Lambda_N). \quad (5)$$

The fixed points of this recurrence are at  $\Lambda_1^* = -1$  and  $\Lambda_{\pm}^* = (3 \pm \sqrt{17})/4$ . Only the fixed point  $\Lambda_+^* = \Lambda$  is positive and therefore physically acceptable. This fixed point is also attractive, so that  $D_N/U_N \rightarrow \Lambda$ . Thus, on the three-

coordinated tree there are  $\Lambda \approx 1.7808$  times more metastable states with determined root spin than with undetermined root spin.

To determine  $D_N$  we iterate  $D_N = D_{N-1}^2 \Lambda_N$  to give

$$D_N = (D_1)^{2^{N-1}} \prod_{k=2}^N (\Lambda_k)^{2^{N-k}}. \quad (6)$$

This equation implies that  $D_N \propto \delta^{2^N}$  with

$$\delta = \lim_{N \rightarrow \infty} (D_N)^{2^{-N}} = (D_1)^{1/2} \prod_{j=2}^{\infty} (\Lambda_j)^{2^{-j}}. \quad (7)$$

From Eqs. (3) and (4), and with initial conditions  $D_0=0$  and  $U_0=2$ , we obtain  $D_1=2$  and  $\Lambda_2=1/2$ . Using these values and the recurrence (5) we numerically determine  $\delta = 1.5658 \dots$ .

To complete the derivation of  $D_N$  and  $U_N$  we employ Eqs. (6) and (7) to find the exact expression for the ratio

$$\delta^{2^N} / D_N = \prod_{j=1}^{\infty} (\Lambda_{j+N})^{2^{-j}}. \quad (8)$$

Since  $\Lambda_N \rightarrow \Lambda$ , the product on the right-hand side of Eq. (8) approaches  $\Lambda$  as  $N \rightarrow \infty$ . Together with the fact that  $D_N/U_N \rightarrow \Lambda$ , we obtain

$$D_N \rightarrow \Lambda^{-1} \delta^{2^N}, \quad U_N \rightarrow \Lambda^{-2} \delta^{2^N}. \quad (9)$$

These results should be compared to the total number of the spin states  $S_N = 2^{\mathcal{N}}$ , where  $\mathcal{N} = 2^{N+1} - 1$  is the total number of sites in the three-coordinated  $N$ -level tree. The entropy of the number of metastable states,  $\ln(U_N + D_N)$ , grows asymptotically as  $C\mathcal{N}$ , with  $C = \frac{1}{2} \ln \delta \approx 0.2242$ . The linear  $\mathcal{N}$  dependence fits with the previous lower bound according to which the metastable state entropy increases as  $\mathcal{N}^{1-1/d}$  in  $d$  dimensions.

#### IV. FINITE TEMPERATURE

For a system that is quenched from infinite to low but nonzero temperature, equilibrium is eventually reached. However, the approach to equilibrium proceeds in two distinct stages. In the initial stage, the evolution is essentially the same as that of the zero temperature case. Thus in two dimensions the system first relaxes to a metastable stripe state with probability  $\approx 1/3$ . This would be the final state at zero temperature. At finite temperature, however, there is a slow escape from this metastable state whose rate we now determine by a simple geometric approach (Fig. 13).

The disappearance of a stripe occurs by the following steps. First, a dent is created by flipping a spin at a domain wall. The time required for this event is of the order of  $e^{4J/T}$ , where  $4J$  is the energy cost associated with the spin flip. Once a dent is created, the spin at the dent, as well its two vertical neighbors, are now free to flip. This gives rise to diffusive motion for the two horizontal segments of the dent. Thus the vertical length of the dent performs a one-dimensional random walk which terminates when the horizontal segments meet.

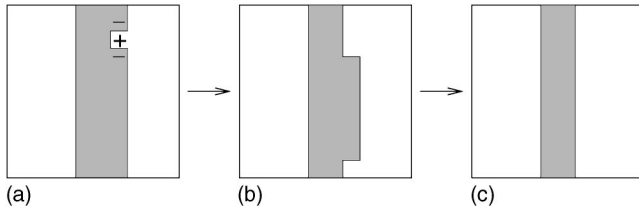


FIG. 13. Relaxation of a stripe state in two dimensions at small nonzero temperature: (a) nucleation of a dent (freely flippable spins are indicated); (b) diffusive growth of the dent; (c) dent reaches the system size and hence the domain wall steps to the left. This overall process ultimately leads to the disappearance of the stripe.

From elementary facts about the first passage of a one-dimensional random walk in the presence of an absorbing boundary [17], the dent recombines with probability  $(L-1)/L$  and the domain wall returns to its original state, while with probability  $1/L$  the dent expands and ultimately changes the sign of one column of spins. Thus we need  $L$  dent creation events before the stripe width changes by  $\pm 1$ . The time needed for this event is of order  $L e^{4J/T}$ . Since the typical width of a stripe is of the order of  $L$ , there must typically be  $L^2$  such stripe width hopping events before two interfaces meet and annihilate. Thus the time for a stripe state to disappear is of order  $\tau \sim L^3 e^{4J/T}$ . This time scale greatly exceeds the formation time (of order  $L^2$ ) to form a stripe during the initial zero-temperature relaxation stage [4], so that the asymptotic behavior is controlled by  $\tau$ .

Our simulations agree with this prediction even up to  $T/T_c \leq 0.2$  (Fig. 14). Here we define the relaxation time as the time for the system to first reach the equilibrium value of the magnetization of the Ising model at temperature  $T$ . This relaxation time is dominated by configurations that first reach a stripe state; configurations that avoid the stripe state relax to equilibrium much more quickly.

We can develop a similar argument in three dimensions. Since a typical metastable state has the form of two interpenetrating three-arm stars, let us estimate the time for such a structure to disappear. The lowest energy excitation is to flip of the order of  $L^2$  spins in a planar region to complete an  $L \times L$  slab of aligned spins. This excitation then relaxes relatively more quickly to the ground state. The time needed to create this planar barrier scales as  $\exp(4JL^2/T)$ . However, this

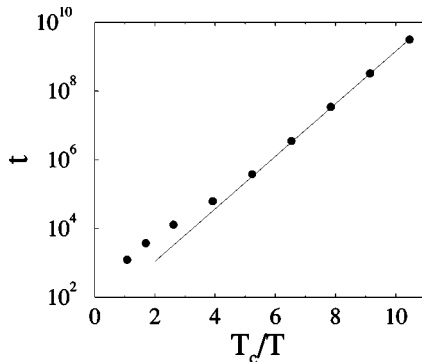


FIG. 14. Time to reach the equilibrium state on the square lattice. The straight line is  $L^3 e^{4J/T}$ .

time is too long to observe this relaxation mechanism by direct simulations.

## V. SUMMARY AND DISCUSSION

Our main result is that a finite homogeneous Ising ferromagnet with Glauber kinetics generally does not reach the ground state when it is quenched to zero temperature. In two dimensions, the final state can be either the ground state or a frozen stripe phase. It is not *a priori* obvious which of these possibilities can occur in the thermodynamic limit. Our simulations indicate that for zero initial magnetization the probability of ending in a stripe phase is close to  $1/3$ . We also argued that  $k$ -stripe states occur with probability  $P_k > 0$  for even  $k$ , with  $P_k \sim e^{-k^2}$  as  $k \rightarrow \infty$ . A rigorous proof of these results represents a fundamental challenge.

We also tested the universality of our findings by considering different lattices and different boundary conditions. While these changes slightly affect various quantitative results (see Fig. 1), they do not affect our major conclusions. We also checked that starting from a specific initial condition (for example, the antiferromagnetic initial state) and averaging only over different realizations of the dynamics gives essentially identical results to those where we consider one realization of the dynamics for each initial spin state.

A more fundamental test of universality is to consider systems with different dynamical rules that still belong to the universality class of nonconserved order-parameter dynamics. The phase-ordering kinetics of a generic two-phase system with a nonconserved scalar order parameter is generically described by a time-dependent Ginzburg-Landau (TDGL) equation [2]. In the absence of thermal noise this dynamics is deterministic, while Glauber dynamics is stochastic even at zero temperature. Despite this distinction both dynamics lead to similar final states in two dimensions, viz., TDGL dynamics leads to a stripe state in approximately 30% of the realizations. Strictly speaking, the stripe state is not absolutely stable with respect to the TDGL dynamics: A straight stripe of width  $W$  disappears on a time scale of the order of  $e^W$ , as follows from the analysis of the one-dimensional TDGL equation [18]. For a macroscopic system and when  $W$  is of the order of  $L$ , the relaxation time  $e^W \sim e^L$  is “infinite” in any practical sense. Thus, the appearance of stripes in the TDGL equation indicates that this geometrical feature should appear ubiquitously in the low-temperature relaxation of two-dimensional spin systems with nonconserved dynamics.

In spatial dimensions  $d \geq 3$ , the probability that the system reaches either the ground state or a frozen state is vanishingly small (again in the most relevant case of zero initial magnetization). Essentially all realizations end up wandering forever on connected isoenergy sets of blinker states. The existence of blinkers means that the  $d \geq 3$  kinetic Ising-Glauber system belongs to the mixed type according to the Newman-Stein classification [3]. That is, a fraction of the spins flip infinitely often (those on blinkers), while the rest of the spins flip a finite number of times.

Blinkers appear to be a general feature of discrete-state ferromagnets. For example, they arise readily in the  $q$ -state



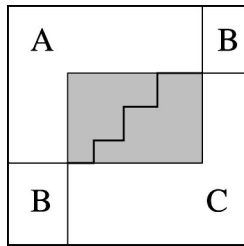


FIG. 15. Generic blinker in the kinetic three-state Potts model on the square lattice. The shaded region can flip between all spins in the A and C states. The remaining spins are stable since they have at most one misaligned neighbor. A typical position of the AC interface in the shaded region is shown (thick line).

Potts model with Glauber kinetics, even in two dimensions. Here zero-temperature Glauber kinetics means that a spin flips to agree with the majority of its neighbors. In cases of a “tie,” that is, if half the neighbors of a given spin are in one state and the other half are in another state, then the spin flips to one of these states equiprobably. For the three-state Potts model on the square lattice with equal initial concentrations of all three states, blinker states of the form illustrated in Fig. 15 typically arise. The shaded region can blink between all spins in the A or the C states. While it was previously argued that domains become pinned for quenches to  $T=0$  when  $q \geq 3$  [10], our simulations of the three-state Potts model indicate that the probabilities of reaching the ground state and a frozen state decrease with increasing system size  $L$  and approach zero as  $L \rightarrow \infty$ . In short, the Potts system gets pinned in a blinking state rather than in a frozen state.

One reason that the system does not reach the ground

state is that metastable states become more numerous as the spatial dimension increases. We argued that the number of these metastable states scales as  $\exp(\mathcal{N}^{1-1/d})$  in  $d$  dimensions, where  $\mathcal{N}$  is the total number of spins. Thus a spin system is increasingly likely to first encounter and get trapped in a metastable state before the ground state can be reached as the dimension increases. Associated with the metastable states are a variety of interesting and unexplained features, such as the distribution of magnetization and the distribution of energy. The determination of the number of metastable states for  $d \geq 3$  also appears to be a deep enumeration problem.

At low temperature, the Ising-Glauber ferromagnet necessarily reaches equilibrium, but via a two-stage relaxation process. Initially, the kinetics is nearly identical to that of the zero-temperature case. For those systems that reach a metastable stripe state in two dimensions, there is then a slow approach to equilibrium by the nucleation of defects which cause the stripe boundaries to diffuse, ultimately merge, and thus disappear. Because this kinetics is an activated process, the equilibration time is extremely long and scales as  $L^3 e^{J/T}$ . Surprisingly, this two-stage picture persists for temperatures up to  $0.2T_c$  in two dimensions. A similar picture arises in higher dimensions, but with astronomically long time scales associated with surmounting metastable barriers and reaching equilibrium.

#### ACKNOWLEDGMENTS

We are grateful to NSF Grant No. DMR9978902 for partial support of this work. We also thank A. Lipowski for helpful correspondence and J. Sethna for informative discussions and advice about visualization.

- 
- [1] R.J. Glauber, *J. Math. Phys.* **4**, 294 (1963).
  - [2] J.D. Gunton, M. San Miguel, and P.S. Sahni, in *Phase Transitions and Critical Phenomena*, edited by C. Domb and J.L. Lebowitz (Academic, New York, 1983), Vol. 8; A.J. Bray, *Adv. Phys.* **43**, 357 (1994).
  - [3] C.M. Newman and D.L. Stein, *Phys. Rev. Lett.* **82**, 3944 (1999); *Physica A* **279**, 159 (2000).
  - [4] A preliminary account of this work is given in V. Spirin, P.L. Krapivsky, and S. Redner, *Phys. Rev. E* **63**, 036118 (2001).
  - [5] See, e.g., T.M. Liggett, *Interacting Particle Systems* (Springer-Verlag, New York, 1985).
  - [6] J. Chalupa, P.L. Leath, and G. Reich, *J. Phys. C* **12**, L31 (1979); P.M. Kogut and P.L. Leath, *ibid.* **14**, 3187 (1981); J. Adler, *Physica A* **171**, 453 (1991).
  - [7] D. Stauffer and A. Aharony, *Introduction to Percolation Theory* (Taylor & Francis, London, 1992).
  - [8] Anomalies associated with stripes and other metastable states have been hinted at in [9] for the Ising models and in [10] for the Potts models.
  - [9] E.T. Gawłinski, M. Grant, J.D. Gunton, and K. Kaski, *Phys. Rev. B* **31**, 281 (1985); J. Viñals and M. Grant, *ibid.* **36**, 7036 (1987); J.D. Shore, M. Holzer, and J.P. Sethna, *ibid.* **46**, 11376 (1992); J. Kurchan and L. Laloux, *J. Phys. A* **29**, 1929 (1996); D.S. Fisher, *Physica D* **102**, 204 (1997); A. Lipowski, *Physica A* **268**, 6 (1999).
  - [10] I.M. Lifshitz, *Zh. Exp. Theor. Fiz.* **42**, 1354 (1962) [*Sov. Phys. JETP* **15**, 939 (1962)]; S.A. Safran, P.S. Sahni, and G.S. Grest, *Phys. Rev. B* **28**, 2693 (1983); P.S. Sahni, D.J. Srolovitz, G.S. Grest, M.P. Anderson, and S.A. Safran, *ibid.* **28**, 2705 (1983).
  - [11] P. Sen, *Int. J. Mod. Phys. C* **8**, 229 (1997); **10**, 747 (1999); P. Grassberger and W. Nadler, e-print cond-mat/0010265.
  - [12] M. Aizenman, *Nucl. Phys. B* **485**, 551 (1997); J. Cardy, *J. Phys. A* **31**, L105 (1998).
  - [13] S. Redner, *J. Stat. Phys.* **25**, 15 (1981).
  - [14] P. Svenson, *Phys. Rev. E* **64**, 036122 (2001).
  - [15] D.S. Dean, *Eur. Phys. J. B* **15**, 493 (2000); A. Lefevre and D.S. Dean, *ibid.* **21**, 121 (2001).
  - [16] A detailed study of this glassy behavior on the Cayley tree is given by R. Mélin, J. C. Anglès D’Auriac, P. Chandra, and B. Douçot, *J. Phys. A* **29**, 5773 (1996).
  - [17] S. Redner, *A Guide to First-Passage Processes* (Cambridge University Press, New York, 2001).
  - [18] K. Kawasaki and T. Nagai, *Physica A* **121**, 175 (1983); T. Nagai and K. Kawasaki, *ibid.* **134**, 483 (1986).